

Does Water Scarcity Shift the Electricity Generation Mix toward Fossil Fuels?

*Empirical Evidence from the
United States*

Jonathan Eyer and Casey J. Wichman

1616 P St. NW
Washington, DC 20036
202-328-5000 www.rff.org

Does water scarcity shift the electricity generation mix toward fossil fuels? Empirical evidence from the United States*

Jonathan Eyer¹ and Casey J. Wichman²

¹University of Southern California

²Resources for the Future

September 27, 2016

Abstract

Water withdrawals for the energy sector are the largest use of fresh water in the United States. Using an econometric model of monthly plant-level electricity generation levels between 2001 and 2012, we estimate the effect of water scarcity on the US electricity fuel mix. We find that hydroelectric generation decreases substantially in response to drought, although this baseline generation is offset primarily by natural gas, depending on the geographic region. We provide empirical evidence that drought can increase emissions of CO₂ as well as local pollutants. We quantify the average social costs of water scarcity to be \$51 million per state-year (2015 dollars) attributable to CO₂ emissions alone; however, this figure is much larger for regions that rely heavily on hydropower.

Keywords: water scarcity, electricity generation, CO₂ emissions, air pollution, climate change

JEL Codes: Q41, Q53, Q51, Q25, L94, D22

*Eyer: jeyer@usc.edu. Wichman: wichman@rff.org. We are grateful to Maureen Cropper, Karen Palmer, Robertson C. Williams III, Edson Severnini, Paul Ferraro, Ujjayant Chakravorty, Timothy Hamilton, Peter Maniloff, and Patrick Walsh for helpful discussions and comments. This paper also benefited from suggestions from seminar and conference participants at Resources for the Future, EPA's National Center for Environmental Economics, the 2016 American Economics Association annual meeting, the 2015 Association of Environmental and Resource Economists meeting, the 2015 Agricultural and Applied Economics Association meeting, and the 2014 Southern Economics Association meeting. Brandon Cunningham provided exceptional research assistance. Previous versions of this paper were circulated using the title, "The effect of water supply shocks on the electricity generation mix: Implications for climate change."

1 Introduction

Water withdrawals by power plants are the single largest use of fresh water in the United States (Kenny et al., 2009). Because power plants require water for electricity generation, either to turn hydroelectric turbines or to cool steam (Macknick et al., 2012a), increased water scarcity may induce reductions in generation from relatively water-intensive power plants toward less-water-intensive plants for a number of reasons. Most directly, decreased water availability limits generation from hydroelectric power plants (Department of Energy, 2009; van Vliet et al., 2012; Muñoz and Sailor, 1998). Other less direct mechanisms include changes in thermal efficiency associated with higher river temperatures (Linnerud et al., 2011) and higher marginal costs associated with curtailing water use (Maulbetsch and DiFilippo, 2006; McDermott and Nilsen, 2014). Additionally, water needs vary among power plants based on fuel type and characteristics such as cooling technologies and pollution abatement technologies (Newmark et al., 2010; Meldrum et al., 2013; Feeley III et al., 2008; Averyt et al., 2011). As a result, the prevailing mix of fuel sources, cooling technologies, and water sources used for electricity generation may be impacted by changes in water availability, but their market and non-market impacts are not well identified.

Climate change poses immediate risks to supplies of fresh water for the production of electricity as drought becomes more frequent and more severe (Dai, 2011; van Vliet et al., 2012; Koch and Vögele, 2009; Macknick et al., 2012b; Olmstead, 2014; Schewe et al., 2014; Vörösmarty et al., 2000). Several studies estimate the effect of water supply shocks on electricity production, but this literature, generally, is limited by modeling frameworks and assumptions (Bell et al., 2014), narrow geographic focus of analyses (Yates et al., 2013; Madani and Lund, 2010; Flores-López and Yates, 2013), and restricted thematic scope (Macknick et al., 2012a; Meldrum et al., 2013; Muñoz and Sailor, 1998; Scanlon et al., 2013).

There is, however, an economics literature that estimates the change in heating and cooling energy use as temperatures rise dating back to the early 1990s (Baxter and Calandri, 1992; Rosenthal et al., 1995). In recent years, this question has been asked with increasingly

novel data and methods with implications for human adaptation. Deschênes and Greenstone (2011), Barreca et al. (2016), and Aroonruengsawat and Auffhammer (2011), for example, estimate energy consumption using state-level and household-level panels, respectively, to examine how consumers adapt to rising temperatures.¹ Little effort, however, has been given to examining the role of water scarcity in this capacity.

In this paper, we build upon insights from an evolving literature that econometrically estimates the effect of weather fluctuations on economic activity to predict damages from climate change (Dell et al., 2014, 2012; Burke et al., 2015; Hsiang et al., 2013; Schlenker and Roberts, 2009; Barreca et al., 2016; Carleton and Hsiang, 2016). Specifically, we estimate a reduced-form panel data model of plant-level electricity generation across the United States to uncover a relationship between water scarcity and electricity production. To our knowledge, this is the first representative econometric analysis of the vulnerability of the electricity sector to changes in water scarcity. We do not attempt to decompose the avenues through which drought may affect electricity systems. Instead, we acknowledge that the various causal mechanisms may be interdependent and we estimate the aggregate effect of water scarcity on the electricity mix, including associated feedbacks among the mechanisms.

We investigate the effect of variation in water scarcity on plant generation using two related econometric approaches. First, we construct a panel of monthly electricity generation from nearly every power plant in the United States that was in operation between 2001 and 2012, inclusive. Using a linear fixed effects panel data model and controlling for weather shocks which influence electricity demand, we explain the degree to which residual variation in generation decisions can be attributed to changes in the Palmer Drought Severity Index (PDSI), our proxy for water scarcity (see Figure 1) (Alley, 1984). While the PDSI is not directly related to electricity production, it correlates strongly with river flows and precipitation, which are in turn correlated with water temperature, which limits the thermal efficiency of power plants and triggers environmental protection regulations. It is commonly

¹See Auffhammer and Mansur (2014) for a review of the empirical demand-side literature.

used to project the effect of climate change on water availability (Dai, 2011). Moreover, PDSI provides a measure of water scarcity that is comparable throughout the country, abstracting away from the spatial variation in water-electricity mechanisms (e.g. storage, snow pack reliance) and allowing for a national assessment of the link between water scarcity and electricity. Throughout our study period, we capture several severe droughts that vary spatially. During each drought, some regions experience no drought or even water abundance, which aids in identification. An important takeaway is that the PDSI level moves independently of measures of temperature. Because drought is a medium-term trend, its effect on electricity generation will be differentiated from weather patterns and seasonal demand shocks. This fact is central to our identification strategy: conditional on seasonal trends, temperature, and other demand shocks, the effect of changes in water scarcity on electricity generation is a plausibly exogenous shock to supply.

By exploiting data on observable characteristics of power plants, we estimate the heterogeneous effects of water availability on plant generation decisions at plants of different characteristics. Specifically, we focus on the type of water source on which the plant generally relies and the type of technology that thermal power plants use to cool water prior to discharge. Second, in order to account for water scarcity-induced changes in generation along unidentifiable plant dimensions, we directly estimate CO₂, NO_x, and SO₂ emissions from the electricity sector as a function of water availability.

2 Background

The effect of water scarcity on the electricity mix and on emissions depends on the extent to which incumbent electricity generators are susceptible to changes in water supplies as well as the availability and type of alternative generation sources (Meldrum et al., 2013). Electricity in the United States can be transported within three multistate interconnections: Western,

Texas, and Eastern.² The composition of the electricity fleet in each interconnection differs because of such factors as historical accessibility to fuels and local and regional regulations (Table 1). In addition, water sources and cooling technologies vary among interconnections (Table 2). As a result, there is heterogeneity in both the exposure of the existing generation mix to water scarcity and in the type of power plant that will replace generation from water-intensive plants (Graff Zivin et al., 2014). This heterogeneity in turn suggests that the effect of water scarcity on pollutant emissions will vary throughout the country (Muller and Mendelsohn, 2009).

Adaptation to water scarcity for thermoelectric power plants depends critically on available cooling technologies and water sources. A recent review by Macknick et al. (2012a) surveyed water consumption and withdrawal needs for a range of power plant types.³ Among nonrenewable sources, nuclear is generally the most water intensive, followed by coal and then natural gas. Hydroelectric generation and concentrated solar are the most water consumptive renewable electricity sources, while water needs for solar photovoltaic and wind are negligible. Water consumption also varies by cooling type. Water needs in plants using once-through cooling are much lower than those using cooling towers or ponds. Averyt et al. (2011) also document the vulnerability of power plants differentiated by water source. Surface water withdrawals from rivers, lakes, and oceans accounted for nearly all of the water (84 percent) used for thermoelectric thermoelectric cooling. Further, Newmark et al. (2010) note that additional environmental controls, particularly carbon capture and storage (CCS) systems, also increase water needs. Therefore, to the extent that water constraints lead to electricity responses, these responses may occur at both the interfuel and intrafuel level.

Such responses carry environmental and climatological implications. According to a summary of life-cycle fuel analyses by Moomaw et al. (2011), nuclear, hydroelectric, and

²Electric utilities in each of the interconnections are connected electrically during normal system conditions and operate at a synchronized frequency.

³There is an important distinction in water use between withdrawals and consumption. Water withdrawals indicate uses of water that are diverted or withdrawn but returned to their original source, whereas water consumption is the use of water that is not returned to its source due to evaporation, transpiration, physical consumption, or similar processes.

renewable generation emits virtually no carbon dioxide (CO_2), whereas natural gas and coal emit 470 grams per kilowatt-hour (g/kWh) and 840 g/KWh, respectively. CO_2 emissions from natural gas and coal generation can be reduced if the plant operates a CCS system. Similarly, according to the EPA's Emission and Generated Resource Integrated Database (eGRID), nuclear, hydroelectric, and renewable generation emits negligible quantities of sulfur dioxide (SO_2) and nitrogen oxides (NO_x). Coal emits substantial amounts of both SO_2 and NO_x , whereas natural gas emits little SO_2 and approximately one-third the NO_x emissions of coal generation. If water scarcity reduces generation from nuclear, hydroelectric, or renewable sources in favor of coal or natural gas, emissions will rise. On the other hand, if water scarcity shifts generation from coal to natural gas, emissions will decline. Further, heterogeneity in water intensity within a given fuel type allows for yet another margin on which generation could affect emissions. We document evidence of fuel switching and corresponding changes in CO_2 , SO_2 , and NO_x that vary geographically in response to increasing water scarcity.

3 Data

We use several publicly available data sources in our empirical analysis. The first, used in our plant-level analysis, is a nearly comprehensive compilation of electricity generation in the United States for plants operating throughout 2001 and 2012. The second, used in our aggregate analysis, is a combination of state-level emissions data from electricity producers in the US Environmental Protection Agency's (EPA) Air Markets Program (AMP) paired with climatic variables. Paramount to our empirical analyses, we merge water scarcity data at the climate region level within both of our analyses. We aggregate each data source to the monthly level; our analysis spans 2001 to 2012 inclusive. By constructing a large panel in both dimensions, our empirical approach exploits rich cross-sectional and temporal variation.

3.1 Plant-level generation

Monthly net generation data are obtained from Energy Information Administration (EIA) and Federal Energy Regulatory Commission (FERC) forms.⁴ Following the EIA’s categorization, fuel sources are designated as coal, natural gas, petroleum, hydropower, nonhydro renewables (i.e., nuclear, solar, wind, geothermal, biomass), and all other fuel sources. These data span January 2001 through December 2012.

Prior to 2008, information on net generation came from EIA-906, EIA-920, and FERC-423 forms. From 2008 onward, the information was consolidated onto the EIA-923 form. The data were merged from each form using a generator-specific identifier. The EIA-923 contains detailed information on primary fuel sources, prime movers, nameplate capacity, fuel cost receipts, location, and other generator-specific information.

The first and last year that each plant appeared on the EIA-923 is tabulated. For each generator, the sample is restricted to include only those plants that were in operation for the full timespan as indicated by EIA reports. We thus construct a balanced panel because modeling the opening and closing of plants explicitly is beyond the scope of this analysis; however, we do include plants that close for maintenance.

We examine spatial heterogeneity by conditioning our analysis on regional electricity interconnections that define three broad electricity markets within the US. The three interconnections are Western, Texas, and Eastern. The Western interconnection incorporates all electricity produced, roughly, west of the Rocky Mountains. The Texas interconnection incorporates the majority of the state of Texas. The Eastern interconnection encompasses all other generators. Some electricity does move between interconnections, but this fraction is relatively small. Since we are interested primarily in generation decisions in response to local weather conditions, we do not model electricity transmission across the boundaries of the interconnections.

Generation is aggregated by fuel type within each plant. For example, if an operating

⁴Net generation is total generation less generation used for plant operations.

plant maintains two coal-fired generators and three natural gas-fired generators, generation from both coal generators is aggregated and treated as a single plant-by-fuel-type observation. Additionally, the three natural gas generators are aggregated to a single monthly generation observation. Generation arising from different fuel sources within the plant are treated as independent observations.

3.2 Emissions data

Monthly emissions data are obtained from EPA’s Air Markets Program data. The AMP data include hourly information on CO₂, SO₂, and NO_x emissions for every power plant that is subject to an air markets program. Emissions are aggregated to the state-month level to match the climatic data; for the state-level analysis, we aggregate weather variables to the state level. The number of plants included in the AMP has increased as additional air markets have been introduced. In 2001, 1,146 plants comprising 3,410 generators were required to report emissions. In 2012, 1,534 plants comprising 4,923 generators were required to report. Emissions in later years of the sample are, therefore, higher than those in early years of the sample, though we control for this in our empirical models.

We match the state-level emissions data with indicator variables constructed for nine climate regions designated by the NCDC. These regions are Northwest (NW), West, Northern Rockies and Plains (Rock), Southwest (SW), South, Upper Midwest (Midwest), Ohio Valley (Central), Southeast (SE), and Northeast (NE). The number of states in each region varies from 2 (West) to 11 (NE), and although climate regions do not correspond to energy markets, they provide a sensible disaggregation of the national electricity market corresponding to similar climate characteristics (Karl and Koss, 1984).⁵

⁵We analyze emissions at the state (regional) level for ease of interpretation, since interconnection regions and state boundaries are imperfectly aligned.

3.3 Water scarcity and weather variables

We obtain monthly water scarcity and climatic variables from the NCDC. Water scarcity is measured using the Palmer Drought Severity Index (PDSI) and defined at the climate region level. The PDSI is a hydrological measure of supply of and demand for soil moisture that captures drought trends. This variable varies roughly in the range $(-9, 9)$ in our sample, with negative values indicating water scarcity and positive values indicating water abundance. A PDSI value of -2 reflects moderate drought, -3 severe drought, and so on.

Temperature information is represented using cooling degree days (CDDs). CDDs are a non-linear measure of how far temperatures are from an ambient indoor reference temperature. The reference temperature is 65 degrees Fahrenheit.

We plot CDDs relative to PDSI over time in Figure 1 for each interconnection. As shown, the seasonal pattern in CDDs varies cyclically. Throughout our study period, we capture several severe droughts that vary spatially. During each drought, some regions experience no drought or even water abundance, which aids in identification. An important takeaway is that the PDSI level moves independently of these measures of temperature. Since drought is a medium-term weather trend, its effect on electricity generation will be differentiated from weather patterns and seasonal demand shocks. This fact is central to our identification strategy: conditional on seasonal trends, temperature, and other demand shocks, the effect of changes in water scarcity on electricity generation is a plausibly exogenous shock to supply.⁶

3.4 Water sources and cooling technologies

Finally, we obtain water sources and cooling technologies used for all power plants in our sample from the Union of Concerned Scientists' UCS EW3 Energy-Water Database.⁷ Using a variety of EIA sources, the UCS database links power plants to water use, water sources, and

⁶Further, there is no reason to believe that reverse causality would bias results within our study. Changes in generation in response to drought that affect carbon emissions are highly unlikely to have a short-run effect on the prevalence or severity of drought.

⁷Union of Concerned Scientists. 2012. UCS EW3 Energy-Water Database V.1.3. www.ucsusa.org/ew3database. Last accessed: April 11, 2014.

cooling technologies within the existing suite of electricity generators in the United States. We merge information from the UCS database to our time series of generation data at the plant-by-generator level to link generation decisions with water use characteristics within a given plant.

In Table 2, we present summary statistics by water source and cooling technology at the plant level. As shown, plants relying on surface water withdrawals constitute the majority of our sample, while municipal and groundwater sources also account for a sizable portion of the distribution. Other sources could contain seawater or wastewater, for example, to cool power plants.

Cooling technologies for each plant are also tabulated in Table 2. The vast majority of plants have no cooling technology reported. These plants could be hydroelectric plants or natural gas combustion turbines, neither of which requires cooling. Recirculating cooling is the next most prevalent cooling type, followed by once-through cooling. Both of these metrics vary across interconnection regions. Cooling ponds and dry cooling towers constitute a smaller share of the cooling technologies used by the plants in our sample.

4 Methodology

Our empirical models exploit the conditional exogeneity of water scarcity as it affects generation and emissions. To that extent, we develop two independent analyses. In the first, we examine the effect of water scarcity on electricity generation at the plant level. We refer to these as our “plant-level” models. Within our plant-level specifications, we analyze the importance of existing, and heterogeneous, capital stock within an electricity market and its ability to react to changes in water scarcity. In the second, we provide a broader analysis of the effect of water scarcity on emissions of air pollutants. We limit this analysis to changes in emissions levels at the state level and, hence, refer to these as our “state-level” models.

4.1 Plant-level models

We identify changes in the United States electricity generation mix attributable to water scarcity econometrically. Our approach differs from the prior literature in which hydrologists and engineers employ either large-scale models that simulate climatic conditions based on a fixed generation stock (e.g., van Vliet et al. (2012); Macknick et al. (2012b)) or narrower analyses that track the full life cycle of water in the production of electricity (e.g., Scanlon et al. (2013)). In contrast, we use observed variation in water scarcity in the United States between 2001 and 2012 to identify changes in electricity generation disaggregated by fuel type and geography. Attribution of causality relies on the extent to which water scarcity shifts electricity supply exogenously after controlling for seasonal trends, temperature, and other contemporaneous demand shocks. Conditional exogeneity of water scarcity, in this context, is a plausible assertion.

To understand plant decisions in response to water scarcity, we estimate the effect of changes in PDSI on plant generation directly. We first specify a baseline panel model of net generation that controls for unobserved plant heterogeneity. Our baseline specification is

$$\sinh^{-1}(\text{NetGen}_{irnt}) = \sum_{k \in K} \delta^k (\text{PDSI}_{rt} \times \text{Fuel}_i^k) + \theta \text{CDD}_{rt} + \mathbf{X}_{\mathbf{rnt}} \gamma + \alpha_i + \tau_t + \varepsilon_{irnt} \quad (1)$$

where NetGen_{irnt} is net generation for plant i in climate region r in interconnection n at time t . An inverse hyperbolic sine transformation (\sinh^{-1}) is applied to net generation. Essentially, \sinh^{-1} can be interpreted the same as a natural logarithm for a positive support and exhibits the desirable property of being defined at 0, since we do have true zero observations in our NetGen_{irnt} variable. The inverse hyperbolic sine transformation is defined as $\sinh^{-1}(x) = \ln(x + (1 + x^2)^{1/2})$ and, except for very small values of x , is approximately equal to $\ln(2x)$. Hence, coefficients can be interpreted as (semi-)elasticities (Burbidge et al., 1988). We interact our drought index (PDSI_{rt}) with an indicator for each plant’s fuel type k in the set of all available fuel types K . CDD_{rt} are cooling degree days at the region-month

level. Plant and time fixed effects are represented by α_i and τ_t . Plant fixed effects absorb any unobservable time-invariant characteristics of the plant, such as nameplate capacity, and allow comparisons among plants of varying sizes. Time fixed effects control flexibly for changes in market characteristics, such as changes in relative fuel prices over time, that are not modeled explicitly because of data limitations. The residual error term (ε_{irnt}) is adjusted for autocorrelation at the plant level.

In the baseline specifications that we consider, we adjust the elements included in \mathbf{X}_{snt} , α_i , and τ_t and observe how our parameters of interest, δ^k , evolve. Specifically, we include some combination of demand controls, including cooling degree days and total generation of electricity within an interconnection. The notion here is that after controlling for plant and time fixed effects, if we fix demand at a given level, we can explain the residual variation in a plant’s generation with variation in our drought indicator. Thus, the set of parameters δ^k provides estimates of the effect of changes in PDSI on plant-level generation conditional on fuel type k .

4.2 Regional heterogeneity

Since water scarcity affects the electricity sector differently depending on the capital stock and generation portfolio in a given energy market, we estimate our preferred models on subsets of the national market. We disaggregate the national market by three regional interconnections that are well-defined geographic markets. The benefit from estimating market-specific heterogeneity lies primarily in identifying the role of fuel switching in the short run, given an existing generation fleet. For the Western interconnection, for example, hydropower accounts for more than 30 percent of total generation and thus will respond differently from the Texas interconnection, which generates less than one percent of its electricity from hydropower (Table 1). Thus, the national plant-level estimates conceal policy-relevant heterogeneity. The limitation of such an approach is that we ignore electricity transmitted across interconnections.

4.3 Drought severity, water sources, and cooling technologies

Thus far, we have limited the relationship between electricity generation and water scarcity to be linear and rather simplistic. We recognize that moderate drought may induce different responses from the electricity sector than catastrophic drought, which is analogous to non-linear effects of temperature on economic activity (Burke et al., 2015). We also rely on the positive—that is, the water-abundant portion—of the PDSI distribution for identification. We are therefore concerned that our results may not fully reflect the extent to which water scarcity affects the generation mix.

We again estimate the inverse hyperbolic sine of net generation at the plant level, modifying our estimating equation as follows:

$$\begin{aligned} \sinh^{-1}(\text{NetGen}_{irnt}) = & \sum_{k \in K} \sum_{b \in B} \delta^{bk} (\text{PDSI}_{rt} \times \text{Bin}_{rt}^b \times \text{Fuel}_i^k) \\ & + \theta \text{CDD}_{rt} + \mathbf{X}_{\text{rnt}} \gamma + \alpha_i + \tau_t + \varepsilon_{irnt}. \end{aligned} \tag{2}$$

We decompose the PDSI distribution into six bins and construct a vector of indicator variables, Bin_{rt}^b , that equal one if a climate region’s PDSI value falls in bin b and zero otherwise. The first bin captures PDSI_{rt} observations below -5 ; the second captures observations for $\text{PDSI}_{rt} \in [-5, -2)$; the third, $\text{PDSI}_{rt} \in [-2, 0)$; the fourth, $\text{PDSI}_{rt} \in [0, 2)$; the fifth, $\text{PDSI}_{rt} \in [2, 5)$; and the sixth, $\text{PDSI}_{rt} \geq 5$. Each bin corresponds, roughly, to drought indicators used widely for communicating drought severity to the public. These models are estimated to provide a sense of how the severity of drought (or water abundance) affects generation from different fuel sources heterogeneously. We recognize that this disaggregation restricts electricity generation to be linear within each bin. We leave a comprehensive analysis of the nonlinearities in the electricity sector’s response to water scarcity, especially catastrophic drought, for future work.

Further, the extent to which an incumbent power plant is susceptible to changes in water scarcity depends on both its water source and cooling technology, both of which remain

fixed for a given plant in our sample. Thus, although our panel estimation controls for this heterogeneity among plants, it also masks how plants with different water sources or cooling technologies might respond to drought differently. To examine heterogeneous responses to water scarcity along these dimensions, we estimate Equation 1 including interactions of $PDSI_{rt}$ with indicator variables for the cooling type and water source of power plant i , respectively. These results provide insight into the vulnerability of different types of power plants while also highlighting ways the electricity sector can adapt to water shortages in the short to medium run.

4.4 State-level models

The primary goal of the state-level models is to put the effects of water scarcity on electricity generation estimated at the plant level into relevant economic terms. Thus, we posit a model of state emissions from electricity generation that depends on our water scarcity index and controls flexibly for weather, time, and time-invariant unobservable characteristics at the state level. Our estimating equation is

$$\ln(\text{emissions}_{st}^j) = \delta PDSI_{st} + \theta CDD_{st} + \alpha_s + \tau_t + \varepsilon_{st}, \quad (3)$$

where emissions_{st}^j is the level of emissions of pollutant type j for $j \in \{\text{CO}_2, \text{NO}_x, \text{SO}_2\}$ in state s during month t . CDD_{st} are cooling degree days as defined previously. α_s and τ_t are state and month-of-sample fixed effects, respectively. And, ε_{st} is the residual error term. $PDSI_{st}$ is the average PDSI level for a state-month observation. We are thus interested in the coefficient δ , as this will identify the effect of changes in water scarcity on realized emissions levels.

The set of fixed effects in Equation 3 plays an important role for identification. α_s captures fixed, time-invariant differences between states, such as the mix of incumbent generators and regional endowments of fuel or water supplies, among other things. τ_t absorbs

common seasonal demand shocks (beyond that of state-specific weather shocks), variation in relative fuel prices that are smoothed throughout the month, changes in abatement technology, and changes in the number of plants covered under the Air Markets Program. Thus, after controlling for weather, state and month fixed effects, and other controls, the residual variation in emissions at the state level that can be explained by PDSI (δ) is the direct effect of water scarcity on emissions from electricity generation.

To explore this further, we disaggregate our national models to identify region-specific effects. Specifically, we estimate Equation 3 with interactions between PDSI and nine climate region indicators. Although these regions do not correspond to the market for electricity supply, they do provide a clean disaggregation of states with similar climatic characteristics (Karl and Koss, 1984). For this reason, we believe these estimates shed light on heterogeneous spatial emissions. We note that for SO_2 and NO_x , both flow pollutants, the damages that arise from electricity production occur reasonably close to their source of generation in both time and space (Muller and Mendelsohn, 2009). Emissions of SO_2 and NO_x also interact with other chemicals and physical processes; thus, we refrain from interpreting changes in emissions of these pollutants as changes in pollution. CO_2 , being a stock pollutant, does not necessarily produce immediate damages in a given geography or time. Thus, our region-specific results identify heterogeneity in the emissions of CO_2 , NO_x , and SO_2 induced by water scarcity in the electricity sector.

5 Results and discussion

Our initial results for the full sample are presented in Table 3. Our empirical results suggest that increases in water scarcity (a decrease in the PDSI) reduce hydroelectric generation substantially. A one standard deviation increase in the PDSI ($\sigma = 2.7$) results in an approximately 27 percent decrease in electricity generation at hydroelectric plants. This forgone hydroelectric generation is offset primarily by natural gas generation, resulting in a net 13.4

percent increase in natural gas generation per standard deviation increase water scarcity. At the national level, there is no statistically significant effect of water scarcity on either renewable or nuclear generation. A similar pattern is shown in Table 4 for the Western and Eastern interconnections: drought-induced reductions in hydropower are offset primarily by increases in natural gas generation. Further, decreases in coal generation in the Eastern interconnection are observed, suggesting potential shifting toward less-water-intensive fossil fuel generation (Macknick et al., 2012a). Because displaced hydroelectric generation is offset by fossil fuel generation rather than renewable or nuclear generation, carbon dioxide emissions from the electricity sector are likely to increase with increases in water scarcity.

As shown in Figure 2, increases in water scarcity reduce generation from hydroelectric sources across the entire distribution of water scarcity in the Eastern and Western interconnections. In both cases, the marginal effect of changes in water scarcity is largest at the driest end of the water scarcity distribution, indicating that a change from moderate drought to extreme drought will reduce hydroelectric generation more than a change from extreme water abundance to moderate water abundance. There is some evidence that increased water scarcity results in decreased hydroelectric generation in the Texas interconnection; however, the results are not consistent throughout the distribution of the PDSI and they possess large confidence intervals. This result is likely due to Texas having very little hydropower. In both the Eastern and Western interconnections, natural gas generation increases as water scarcity increases, with the largest percentage increases occurring at the driest end of the water scarcity spectrum. This result is consistent with the use of natural gas to replace displaced hydroelectric generation.⁸ The effect of water scarcity on coal generation is generally statistically insignificant. There is, however, some evidence in the Eastern interconnection that increased water availability results in increased coal generation along some portion of the water scarcity distribution. This finding is consistent with switching from coal to natural gas electricity sources because of water scarcity because natural gas generators, in general,

⁸As a sensitivity check, we run our primary model specification on the subset of our sample before the natural gas boom, in 2008. Results, presented in Table A1, are similar.

are less water-intensive than coal generators.

Increased water scarcity results in decreases in electricity generation from plants that draw their water from surface water supplies in each of the three interconnections (Table 5). In the Eastern interconnection, reductions in generation from surface water-based plants are met with increased generation from plants that use municipal water or groundwater. In the Western and Texas interconnections, reductions in generation from plants using surface water are primarily met by increases in generation from plants using municipal water and groundwater sources, respectively. In terms of water cooling technology, increases in water scarcity in the Texas and Eastern interconnections result in reductions from plants that do not require water for cooling and plants that use cooling ponds; in these regions water scarcity shifts generation toward plants that use dry cooling (Table 6). In the Western interconnection, increases in water scarcity decrease generation from power plants that do not use water for cooling, and increase generation from plants using once-through cooling, recirculating cooling, or cooling ponds. In our data we observe hydroelectric plants as using no cooling technology, and the effect of water scarcity on generation at plants with no cooling technology is driven by this characterization.

Results from our state-level emissions model suggest that a one-unit decrease in the PDSI at the state level results in an increase in state CO₂ emissions of 1.0 percent, however there are no statistically significant effects of changes in water scarcity on NO_x or SO₂ emissions (Table 7, Panel A). Based on a \$36 per metric ton social cost of carbon (with a three percent discount rate) (Interagency Working Group on Social Cost of Carbon, 2015), the monthly state-level effect of an increase in water scarcity of one standard deviation ($\sigma = 2.7$) is \$4.2 million per state-month (2015 dollars). This value is the equivalent of taking the average state in our sample and moving it from no drought to moderate drought for a single month.⁹

⁹To assign a dollar value to the water scarcity-induced carbon emissions in our sample, we require several pieces of data. First, we take the average value in our sample for CO₂ emissions at the state-month level; this value is 3.83 million metric tons of CO₂ for the full sample. We also use the standard deviation of our drought indicator ($\sigma = 2.7$) to scale our estimated PDSI semi-elasticity from Table 7, Panel A. From this information, we calculate the induced CO₂ emissions to be 103,410 metric tons per state-month. We adopt a \$36 per metric ton estimate of the social cost of carbon (SC-CO₂) with a three percent discount rate

As shown in Figure 3, estimating these social costs of water scarcity in the electricity sector by climate region reveals substantial spatial heterogeneity. Increases in water scarcity in the Northwest climate region (Oregon, Washington, and Idaho) result in large and statistically significant increases in all three measured pollutants, consistent with switching from hydroelectricity to fossil fuels. We estimate the annual social cost of water scarcity-induced CO₂ emissions in the Northwest climate region to be \$78.8 million per state, whereas this number for the West North Central climate region is -\$15 million per state (2015 dollars). Because our pollution estimates do not explicitly consider water scarcity in neighboring climate regions, this result is consistent with power plants in the West North Central climate region offsetting generation in neighboring regions that are affected concurrently by drought. Further, there are smaller but statistically significant increases in CO₂ emissions associated with water scarcity in the South and Southwest climate regions (Table 7, Panel B).

6 Conclusion

In this study, we uncover an effect of changes in water availability on the electricity mix, highlighting the potential short- and mid-term consequences of climate change-induced variation in water scarcity on electricity systems. Further, we identify an important feedback between water scarcity and CO₂ emissions. Still, interpretation of our results for policy purposes is subject to several caveats. First, long-run water scarcity or abundance will affect utility decisions about the construction of new power plants, affecting both the exposure of the electricity mix to water scarcity and the marginal source of electricity generation that will offset displaced generation (Tidwell et al., 2011). Similarly, in our analysis we assume that plant generation and hydroelectric water release decisions are made myopically. If wa-

(2007 dollars), which is intended to monetize the discounted stream of economic damages from an emission of CO₂ Interagency Working Group on Social Cost of Carbon (2015). Using the Bureau of Labor Statistics inflation factor of 1.14, we scale the SC-CO₂ to 2015 dollars. Multiplying each induced CO₂ emission by the SC-CO₂ provides an estimate of the social cost of water scarcity: \$4.2 million (2015 dollars) for the average state-month combination in our sample. It is straightforward to obtain an annual equivalent. We also follow this procedure for regional estimates below.

ter scarcity results in conservation of water sources, our estimates will be overestimated at the beginning of droughts and underestimated at the end of droughts relative to the “true” hydrological production limitation. Still, to the extent that policy is concerned with the response of the electricity mix to water scarcity, the result of interest is, in fact, inclusive of conservation behavior.

Our analysis casts novel light on a key issue at the heart of climate change adaptation—the nexus of water scarcity and the supply of electricity. Further research is needed on the direct implications of water scarcity on water sources and cooling technologies at the plant level, as well as broader studies of the regional, national, and global effects of the ability of the energy sector to adapt to water scarcity.

References

- Alley, William M.**, “The Palmer drought severity index: limitations and assumptions,” *Journal of Climate and Applied Meteorology*, 1984, 23 (7), 1100–1109.
- Aroonruengsawat, Anin and Maximilian Auffhammer**, “Impacts of climate change on residential electricity consumption: evidence from billing data,” in “The Economics of Climate Change: Adaptations Past and Present,” University of Chicago Press, 2011, pp. 311–342.
- Auffhammer, Maximilian and Erin T Mansur**, “Measuring climatic impacts on energy consumption: A review of the empirical literature,” *Energy Economics*, 2014.
- Averyt, K., J. Fisher, A. Huber-Lee, J. Macknick, N. Madden, J. Rogers, and S. Tellinghuisen**, “Freshwater use by U.S. power plants: Electricity’s thirst for a precious resource,” A report of the Energy and Water in a Warming World initiative, Union of Concerned Scientists 2011.
- Barreca, Alan, Karen Clay, Olivier Deschenes, Michael Greenstone, and Joseph S. Shapiro**, “Adapting to Climate Change: The Remarkable Decline in the U.S. Temperature-Mortality Relationship Over the 20th Century,” *Journal of Political Economy*, 2016, 124 (1), 105–159.
- Baxter, Lester W. and Kevin Calandri**, “Global warming and electricity demand: A study of California,” *Energy Policy*, 1992, 20 (3), 233–244.
- Bell, Andrew, Tingju Zhu, Hua Xie, and Claudia Ringler**, “Climate-water interactions—Challenges for improved representation in integrated assessment models,” *Energy Economics*, 2014, 46, 510 – 521.
- Burbidge, John B., Lonnie Magee, and A. Leslie Robb**, “Alternative transformations to handle extreme values of the dependent variable,” *Journal of the American Statistical Association*, 1988, 83 (401), 123–127.
- Burke, Marshall, Solomon M. Hsiang, and Edward Miguel**, “Global non-linear effect of temperature on economic production,” *Nature*, 11 2015, 527 (7577), 235–239.
- Carleton, Tamma A. and Solomon M. Hsiang**, “Social and economic impacts of climate,” *Science*, 2016, 353 (6304).
- Dai, Aiguo**, “Drought under global warming: A review,” *Wiley Interdisciplinary Reviews: Climate Change*, 2011, 2 (1), 45–65.
- Dell, Melissa, Benjamin F. Jones, and Benjamin A. Olken**, “Temperature Shocks and Economic Growth: Evidence from the Last Half Century,” *American Economic Journal: Macroeconomics*, 2012, 4 (3), 66–95.
- , – , and – , “What Do We Learn from the Weather? The New Climate-Economy Literature,” *Journal of Economic Literature*, 2014, 52 (3), 740–98.

- Department of Energy**, “An Analysis of the Effects of Drought Conditions on Electric Power Generation in the Western United States,” Technical Report, United States Department of Energy 2009.
- Deschênes, Olivier and Michael Greenstone**, “Climate change, mortality and adaptation: Evidence from annual fluctuations in weather in the US,” *American Economic Journal: Applied Economics*, 2011, 4 (3), 152–185.
- Feeley III, Thomas J., Timothy J. Skone, Gary J. Stiegel Jr, Andrea McNemar, Michael Nemeth, Brian Schimmoller, James T. Murphy, and Lynn Manfredo**, “Water: A critical resource in the thermoelectric power industry,” *Energy*, 2008, 33 (1), 1–11.
- Flores-López, F. and D. Yates**, “A water system model for exploring electric energy alternatives in southeastern US basins,” *Environmental Research Letters*, 2013, 8 (3), 035041.
- Graff Zivin, Joshua S., Matthew J. Kotchen, and Erin T. Mansur**, “Spatial and temporal heterogeneity of marginal emissions: Implications for electric cars and other electricity-shifting policies,” *Journal of Economic Behavior & Organization*, 2014, 107, 248–268.
- Hsiang, Solomon M., Marshall Burke, and Edward Miguel**, “Quantifying the influence of climate on human conflict,” *Science*, 2013, 341 (6151), 1235367.
- Interagency Working Group on Social Cost of Carbon**, “Technical support document: Technical update of the social cost of carbon for regulatory impact analysis under Executive Order 12866,” Technical Report, United States Government 2015.
- Karl, Thomas R. and Walter James Koss**, “Regional and national monthly, seasonal, and annual temperature weighted by area,” *Historical Climatology Series*, 1984, 4 (3).
- Kenny, Joan F., Nancy L. Barber, Susan S. Hutson, Kristin S. Linsey, John K. Lovelace, and Molly A. Maupin**, *Estimated use of water in the United States in 2005*, US Geological Survey Reston, VA, 2009.
- Koch, Hagen and Stefan Vögele**, “Dynamic modelling of water demand, water availability and adaptation strategies for power plants to global change,” *Ecological Economics*, 2009, 68 (7), 2031–2039.
- Linnerud, Kristin, Torben K. Mideksa, and Gunnar S. Eskeland**, “The impact of climate change on nuclear power supply,” *The Energy Journal*, 2011, 32 (1), 149–168.
- Macknick, J., R. Newmark, G. Heath, and KC Hallett**, “Operational water consumption and withdrawal factors for electricity generating technologies: A review of existing literature,” *Environmental Research Letters*, 2012, 7 (4), 045802.

- , **S. Sattler, K. Averyt, S. Clemmer, and J. Rogers**, “The water implications of generating electricity: Water use across the United States based on different electricity pathways through 2050,” *Environmental Research Letters*, 2012, 7 (4).
- Madani, Kaveh and Jay R. Lund**, “Estimated impacts of climate warming on California’s high-elevation hydropower,” *Climatic Change*, 2010, 102 (3-4), 521–538.
- Maulbetsch, John S. and Michael N. DiFilippo**, “Cost and value of water use at combined cycle power plants,” *California Energy Commission*, 2006.
- McDermott, Grant R. and Øivind A. Nilsen**, “Electricity Prices, River Temperatures, and Cooling Water Scarcity,” *Land Economics*, 2014, 90 (1), 131–148.
- Meldrum, James, Syndi Nettles-Anderson, Garvin Heath, and Jordan Macknick**, “Life cycle water use for electricity generation: a review and harmonization of literature estimates,” *Environmental Research Letters*, 2013, 8 (1), 015031.
- Moomaw, W., P. Burgherr, G. Heath, M. Lenzen, J. Nyboer, and A. Verbruggen**, “Annex II: methodology,” *IPCC special report on renewable energy sources and climate change mitigation*, 2011, pp. 973–1000.
- Muller, Nicholas Z. and Robert Mendelsohn**, “Efficient pollution regulation: Getting the prices right,” *American Economic Review*, 2009, 99 (5), 1714–1739.
- Muñoz, J. Ricardo and David J. Sailor**, “A modelling methodology for assessing the impact of climate variability and climatic change on hydroelectric generation,” *Energy Conversion and Management*, 1998, 39 (14), 1459–1469.
- Newmark, Robin L., Samuel J. Friedmann, and Susan A. Carroll**, “Water challenges for geologic carbon capture and sequestration,” *Environmental Management*, 2010, 45 (4), 651–661.
- Olmstead, Sheila M.**, “Climate change adaptation and water resource management: A review of the literature,” *Energy Economics*, 2014, 46, 500–509.
- Rosenthal, Donald H, Howard K Gruenspecht, and Emily A Moran**, “Effects of global warming on energy use for space heating and cooling in the United States,” *The Energy Journal*, 1995, pp. 77–96.
- Scanlon, Bridget R., Ian Duncan, and Robert C. Reedy**, “Drought and the water–energy nexus in Texas,” *Environmental Research Letters*, 2013, 8 (4), 045033.
- Schewe, Jacob, Jens Heinke, Dieter Gerten, Ingjerd Haddeland, Nigel W. Arnell, Douglas B. Clark, Rutger Dankers, Stephanie Eisner, Balázs M. Fekete, Felipe J. Colón-González et al.**, “Multimodel assessment of water scarcity under climate change,” *Proceedings of the National Academy of Sciences*, 2014, 111 (9), 3245–3250.
- Schlenker, Wolfram and Michael J. Roberts**, “Nonlinear temperature effects indicate severe damages to U.S. crop yields under climate change,” *Proceedings of the National Academy of Sciences*, 2009, 106 (37), 15594–15598.

- Tidwell, Vincent C., Peter H. Kobos, Len A. Malczynski, Geoff Klise, and Cesar R. Castillo**, “Exploring the water-thermoelectric power Nexus,” *Journal of Water Resources Planning and Management*, 2011, 138 (5), 491–501.
- van Vliet, Michelle T. H., John R. Yearsley, Fulco Ludwig, Stefan Vögele, Dennis P. Lettenmaier, and Pavel Kabat**, “Vulnerability of US and European electricity supply to climate change,” *Nature Climate Change*, 2012, 2 (9), 676–681.
- Vörösmarty, Charles J., Pamela Green, Joseph Salisbury, and Richard B. Lammers**, “Global water resources: Vulnerability from climate change and population growth,” *Science*, 2000, 289, 284–288.
- Yates, D., J. Meldrum, F. Flores-López, and Michelle Davis**, “Integrated impacts of future electricity mix scenarios on select southeastern US water resources,” *Environmental Research Letters*, 2013, 8 (3), 035042.

Table 1: Generation statistics by Interconnection

| Fuel type | Percentage of total generation (number of plants) | | |
|-------------|--|---------------|----------------|
| | Western | Texas | Eastern |
| Coal | 35.8% (55) | 42.6% (14) | 59.0% (482) |
| Natural gas | 18.4% (238) | 40.9% (97) | 9.7% (616) |
| Nuclear | 9.5% (3) | 15.0% (2) | 25.2% (58) |
| Petroleum | 0.2% (22) | 0.3% (5) | 1.5% (518) |
| Hydropower | 31.8% (551) | 0.3% (21) | 3.5% (743) |
| Geothermal | 2.4% (44) | – | – |
| Wind | 0.8% (71) | 0.7% (10) | 0.1% (49) |
| Biomass | 0.9% (65) | 0.2% (6) | 0.7% (169) |
| Solar | 0.1% (13) | – | – |
| Other | 0.1% (13) | – | 0.3% (121) |

All statistics presented are percentages for the full sample spanning 2001 through 2012. Percentage of total generation by fuel type is presented along with the number of plants (in parentheses). SOURCE: Authors' calculations.

Table 2: Water source and cooling technology statistics by interconnection

| | Interconnection | | |
|----------------------------|-----------------|-------|---------|
| | Western | Texas | Eastern |
| Water source: | | | |
| Ground | 13.3% | 8.4% | 8.8% |
| Municipal | 12.4% | 15.5% | 13.8% |
| Surface | 55.5% | 52.9% | 55.9% |
| Other | 18.8% | 23.2% | 21.5% |
| Cooling technology: | | | |
| Cooling Pond | 0.6% | 16.1% | 1.8% |
| Dry Cooled | 1.0% | 1.3% | 0.4% |
| Once-Through | 2.1% | 7.1% | 13.5% |
| Recirculating | 17.2% | 30.3% | 14.4% |
| None | 78.0% | 45.2% | 65.5% |
| Other [†] | 1.2% | – | 4.4% |
| No. of plants | 1,075 | 155 | 2,756 |

Entries are proportions of plants with type of water source or cooling technology within each interconnection. The total number of plants in our sample is 3,986. [†] Other cooling type refers to plants for which no cooling type is indicated. SOURCE: Authors' calculations.

Table 3: Baseline regression results

| VARIABLES | (1) OLS | (2) Panel | (3) Panel | (4) Panel | (5) Panel | (6) Panel |
|----------------------------|----------------------|----------------------|----------------------|----------------------|----------------------|----------------------|
| PDSI×Hydro | 0.062*** (0.002) | 0.104*** (0.005) | 0.096*** (0.005) | 0.100*** (0.005) | 0.094*** (0.005) | 0.099*** (0.005) |
| PDSI×Coal | 0.027*** (0.007) | 0.013* (0.007) | 0.013* (0.007) | 0.017** (0.007) | 0.013* (0.007) | 0.016** (0.007) |
| PDSI×Natural gas | -0.144*** (0.004) | -0.048*** (0.006) | -0.055*** (0.007) | -0.049*** (0.007) | -0.055*** (0.007) | -0.049*** (0.007) |
| PDSI×Nuclear | 0.064** (0.027) | 0.016 (0.017) | 0.012 (0.017) | 0.015 (0.017) | 0.011 (0.017) | 0.014 (0.017) |
| PDSI×Solar | 0.245*** (0.023) | 0.039* (0.023) | 0.030 (0.023) | 0.038 (0.023) | 0.031 (0.023) | 0.038 (0.023) |
| PDSI×Wind | -0.038*** (0.005) | 0.012 (0.010) | 0.000 (0.010) | 0.004 (0.010) | 0.001 (0.010) | 0.004 (0.010) |
| PDSI×Geothermal | -0.149*** (0.012) | 0.031 (0.020) | 0.022 (0.019) | 0.029 (0.019) | 0.022 (0.019) | 0.030 (0.019) |
| PDSI×Biomass | -0.054*** (0.006) | -0.016 (0.013) | -0.017 (0.013) | -0.013 (0.013) | -0.018 (0.013) | -0.014 (0.013) |
| PDSI×Petroleum | -0.389*** (0.007) | -0.021*** (0.006) | -0.032*** (0.006) | -0.028*** (0.006) | -0.032*** (0.006) | -0.029*** (0.006) |
| PDSI×Other | 0.116*** (0.013) | -0.037* (0.022) | -0.044** (0.022) | -0.041* (0.022) | -0.045** (0.022) | -0.042* (0.022) |
| CDD | | | | 0.002*** (0.000) | | 0.002*** (0.000) |
| Interconnection generation | | | | | 0.000*** (0.000) | 0.000*** (0.000) |
| Observations | 573,984 | 573,984 | 573,984 | 573,984 | 573,984 | 573,984 |
| No. of plants | 3,986 | 3,986 | 3,986 | 3,986 | 3,986 | 3,986 |
| Within R-squared | 0.013 | 0.006 | 0.033 | 0.036 | 0.034 | 0.036 |
| Plant fixed effects? | N | Y | Y | Y | Y | Y |
| Time fixed effects? | N | N | Y | Y | Y | Y |

The dependent variable in each column is the inverse hyperbolic sine of net generation at the plant level. Column (1) presents results from an ordinary least squares regression. Columns (2)–(6) present results from the “within” fixed effects panel data estimator. “CDD” is cooling degree days. “Interconnection generation” is total electricity generation at the interconnection level. Standard errors in parentheses are clustered at the plant level. *** $p < 0.01$, ** $p < 0.05$, * $p < 0.1$. SOURCE: Authors’ calculations.

Table 4: Fuel type regression results

| | Interconnection | | |
|--------------------------------|----------------------|--------------------|----------------------|
| | Western | Texas | Eastern |
| PDSI×Hydro | 0.087*** (0.009) | 0.062 (0.043) | 0.102*** (0.007) |
| PDSI×Coal | 0.006 (0.021) | -0.038 (0.027) | 0.018** (0.008) |
| PDSI×Natural gas | -0.047*** (0.011) | 0.007 (0.028) | -0.070*** (0.008) |
| PDSI×Nuclear | 0.046 (0.143) | -0.059* (0.030) | 0.014 (0.017) |
| PDSI×Solar | 0.042* (0.024) | | |
| PDSI×Wind | 0.002 (0.013) | -0.048 (0.049) | 0.012 (0.017) |
| PDSI×Geothermal | 0.030 (0.020) | | |
| PDSI×Biomass | -0.023 (0.021) | -0.112* (0.064) | -0.004 (0.017) |
| PDSI×Petroleum | -0.010 (0.031) | 0.065 (0.150) | -0.029*** (0.006) |
| PDSI×Other | 0.084 (0.052) | | -0.062*** (0.024) |
| CDD | 0.002*** (0.000) | | 0.002*** (0.000) |
| Observations | 154,800 | 22,320 | 396,864 |
| No. of plants | 1,075 | 155 | 2,756 |
| Within R-squared | 0.041 | 0.078 | 0.038 |
| Plant fixed effects? | Y | Y | Y |
| Month-of-sample fixed effects? | Y | Y | Y |

The dependent variable in each column is the inverse hyperbolic sine of net generation at the plant level. Standard errors in parentheses are clustered at the plant level. *** $p < 0.01$, ** $p < 0.05$, * $p < 0.1$. SOURCE: Authors' calculations.

Table 5: Water source regression results

| | Interconnection | | |
|--------------------------------|---------------------|----------------------|----------------------|
| | Western | Texas | Eastern |
| PDSI×Surface water | 0.070*** (0.009) | 0.019 (0.030) | 0.043*** (0.005) |
| PDSI×Municipal water | -0.028** (0.014) | 0.006 (0.051) | -0.052*** (0.009) |
| PDSI×Groundwater | 0.003 (0.014) | -0.127*** (0.041) | -0.049*** (0.013) |
| PDSI×Other | -0.007 (0.009) | 0.027 (0.037) | -0.025*** (0.006) |
| CDD | 0.002*** (0.000) | | 0.002*** (0.000) |
| Observations | 154,800 | 22,320 | 396,864 |
| No. of plants | 1,075 | 155 | 2,756 |
| Within R-squared | 0.038 | 0.040 | 0.014 |
| Plant fixed effects? | Y | Y | Y |
| Month-of-sample fixed effects? | Y | Y | Y |

The dependent variable in each column is the inverse hyperbolic sine of net generation at the plant level. Standard errors in parentheses are clustered at the plant level. *** $p < 0.01$, ** $p < 0.05$, * $p < 0.1$. SOURCE: Authors' calculations.

Table 6: Cooling type regression results

| | Interconnection | | |
|--------------------------------|---------------------|-------------------|----------------------|
| | Western | Texas | Eastern |
| PDSI×Once-through | -0.070** (0.027) | 0.047 (0.078) | 0.001 (0.012) |
| PDSI×Recirculating | -0.014 (0.013) | -0.015 (0.035) | -0.004 (0.010) |
| PDSI×Cooling pond | -0.149** (0.064) | 0.049 (0.045) | 0.056*** (0.016) |
| PDSI×Dry cooled | 0.005 (0.019) | 0.319 (0.276) | -0.092 (0.095) |
| PDSI×Other | 0.085 (0.052) | | -0.063*** (0.024) |
| PDSI×None | 0.044*** (0.007) | -0.015 (0.031) | 0.012*** (0.004) |
| CDD | 0.002*** (0.000) | | 0.002*** (0.000) |
| Observations | 154,800 | 22,320 | 396,864 |
| No. of plants | 1,075 | 155 | 2,756 |
| Within R-squared | 0.037 | 0.041 | 0.012 |
| Plant fixed effects? | Y | Y | Y |
| Month-of-sample fixed effects? | Y | Y | Y |

The dependent variable in each column is the inverse hyperbolic sine of net generation at the plant level. Standard errors in parentheses are clustered at the plant level. *** $p < 0.01$, ** $p < 0.05$, * $p < 0.1$. SOURCE: Authors' calculations.

Table 7: State-level emissions results

| | Dependent variable | | |
|--------------------------------------|----------------------|----------------------|----------------------|
| | ln CO ₂ | ln NO _x | ln SO ₂ |
| Panel A: National models | | | |
| PDSI | -0.010** (0.005) | -0.004 (0.007) | -0.004 (0.009) |
| CDD | 0.001*** (0.000) | 0.001*** (0.000) | 0.001*** (0.000) |
| Panel B: NCDC Climate regions | | | |
| PDSI×West | -0.016 (0.021) | -0.033 (0.036) | -0.029 (0.036) |
| PDSI×Northwest | -0.147*** (0.039) | -0.111* (0.063) | -0.127 (0.095) |
| PDSI×Northern Rockies and Plains | -0.004 (0.003) | 0.024*** (0.009) | 0.042*** (0.013) |
| PDSI×Southwest | -0.006*** (0.002) | 0.001 (0.014) | -0.013 (0.014) |
| PDSI×South | -0.014*** (0.003) | -0.027*** (0.006) | -0.046*** (0.010) |
| PDSI×Southeast | -0.005 (0.003) | -0.002 (0.007) | 0.008 (0.009) |
| PDSI×Ohio Valley | -0.001 (0.003) | 0.000 (0.009) | 0.009* (0.005) |
| PDSI×Upper Midwest | 0.004* (0.002) | -0.001 (0.005) | -0.001 (0.007) |
| PDSI×Northeast | -0.003 (0.010) | 0.001 (0.007) | -0.002 (0.024) |
| CDD | 0.001*** (0.000) | 0.001*** (0.000) | 0.001*** (0.000) |
| Observations | 6,912 | 6,912 | 6,911 |
| Number of states | 48 | 48 | 48 |
| State fixed effects? | Y | Y | Y |
| Month-of-sample fixed effects? | Y | Y | Y |

The dependent variable in each column is the natural log of emissions at the state level. Coefficients represent estimation of Equation 3. Standard errors in parentheses are clustered at the state level. *** $p < 0.01$, ** $p < 0.05$, * $p < 0.1$. SOURCE: Authors' calculations.

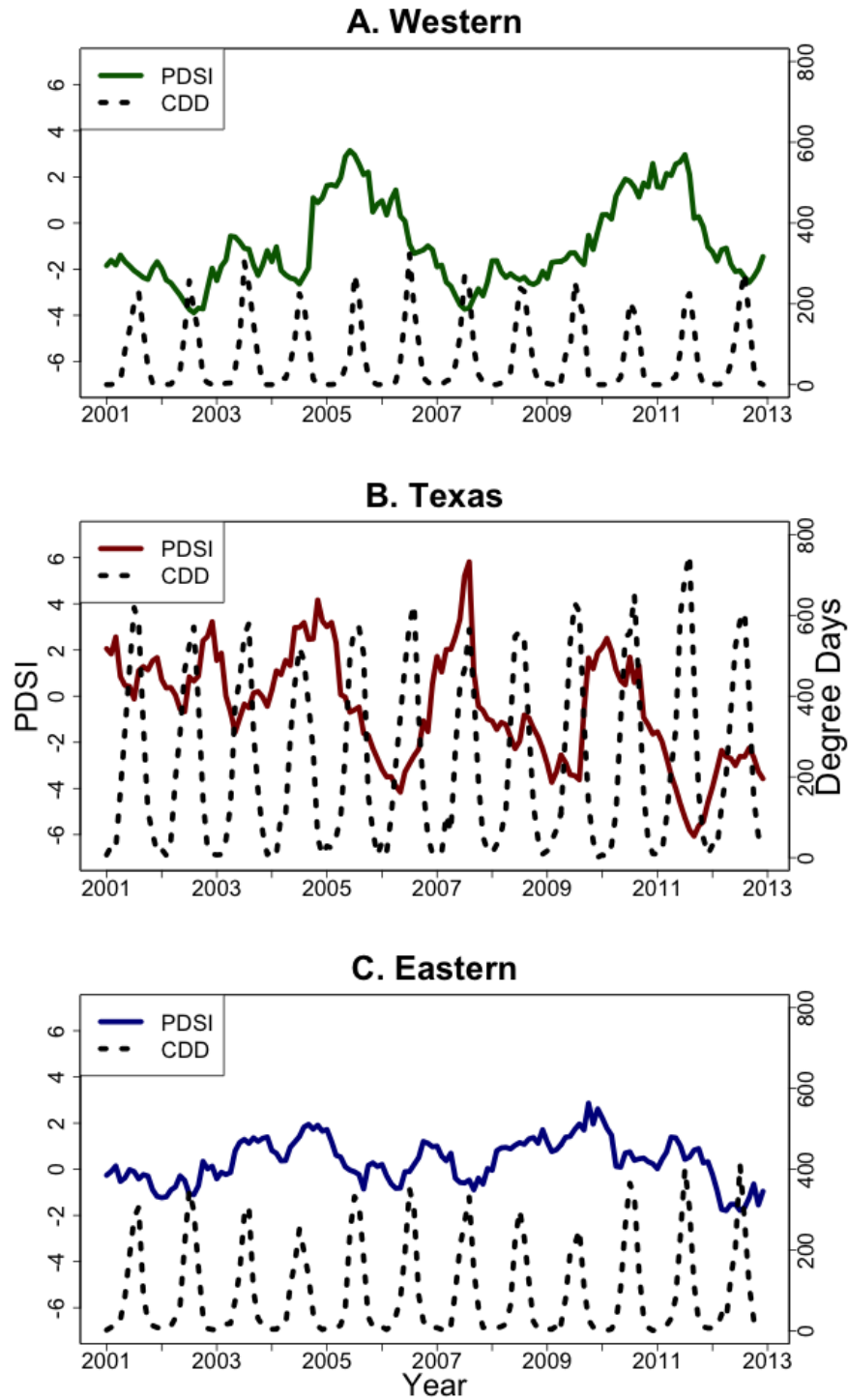


Figure 1: **Palmer Drought Severity Index (PDSI) over time relative to cooling degree days for each interconnection.** Panel A represents temperature and drought variation in the Western interconnection; Panel B represents temperature and drought variation in the Texas interconnection; and Panel C represents temperature and drought variation in the Eastern interconnection.

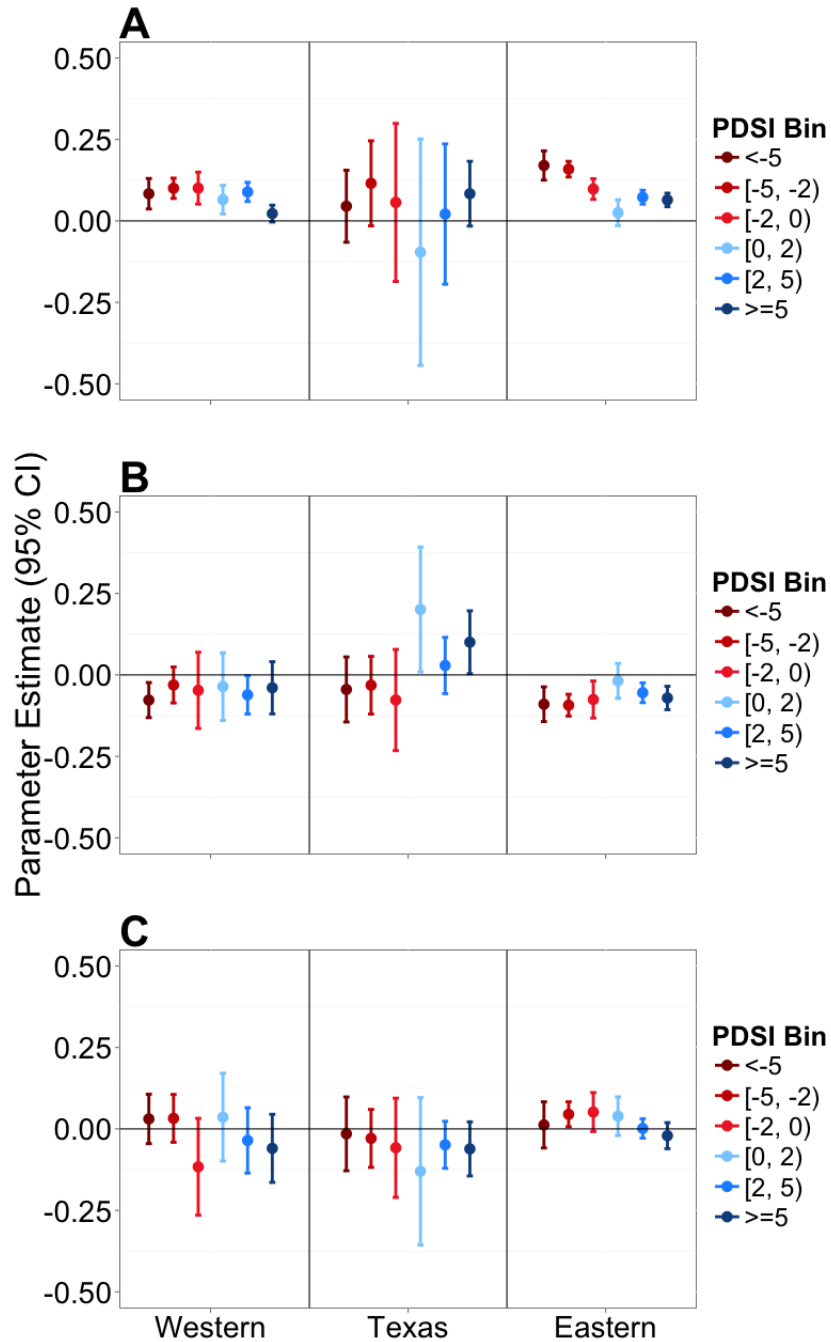


Figure 2: **Heterogeneity in generation by interconnection across the PDSI distribution.** (A) represents hydroelectric generation; (B) represents natural gas generation; and (C) represents coal generation. Estimated coefficients are presented along with 95 percent confidence intervals. Estimates for all three subfigures are obtained from models estimated with two-way fuel type-by-PDSI bin interactions for each interconnection region separately.

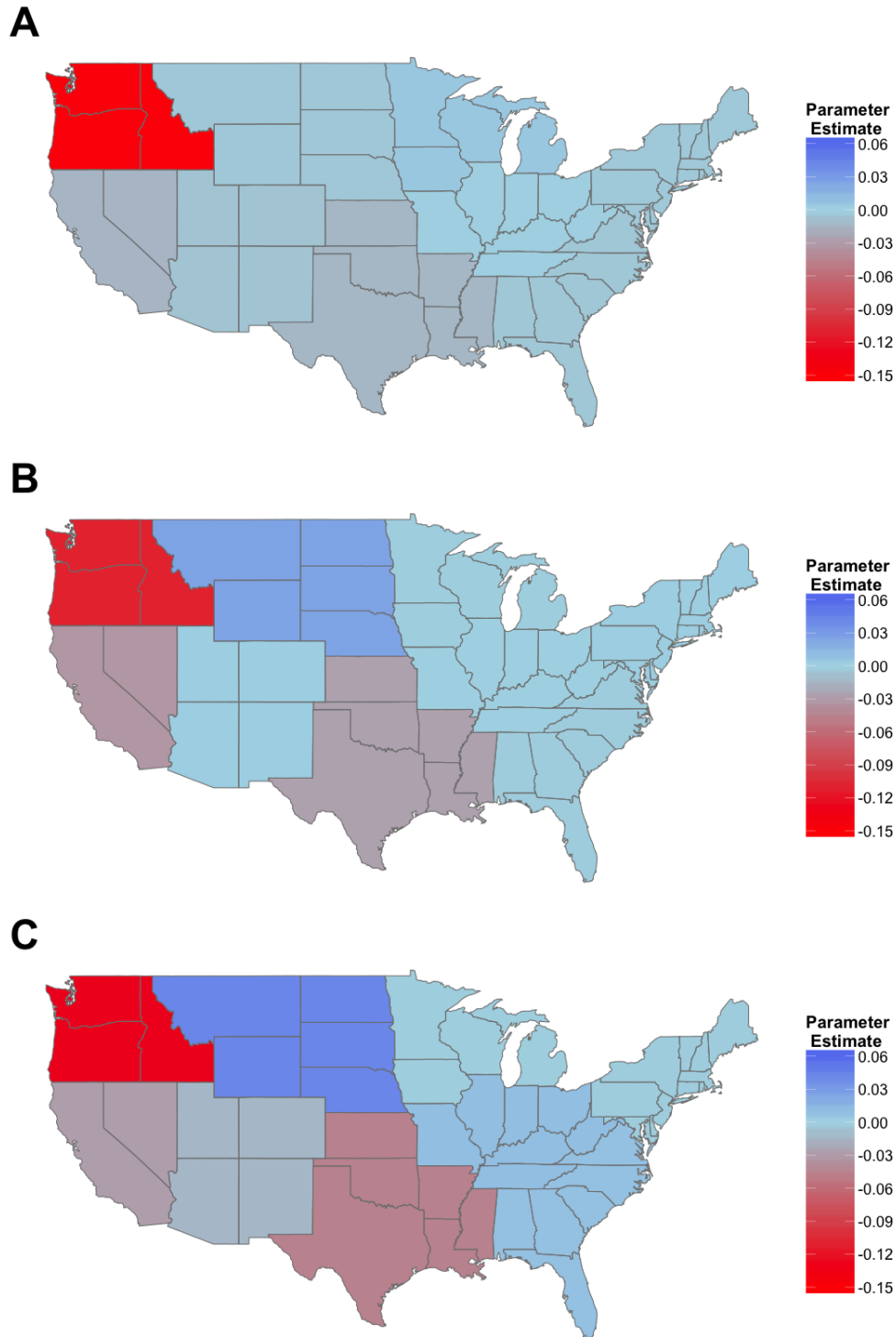


Figure 3: **The effect of water scarcity on state-level CO₂, NO_x, and SO₂ emissions, by NCDC climate region.** (A) represents CO₂ emissions; (B) represents NO_x emissions; and (C) represents SO₂ emissions. Estimated coefficients are presented corresponding to the legend colors.

Appendix A – Additional results

Table A1: Pre-2008 regression results

| | | Interconnection | | |
|--------------------------------|----------------------|---------------------|--------------------|----------------------|
| | | Western | Texas | Eastern |
| PDSI×Hydro | 0.082*** (0.006) | 0.060*** (0.011) | 0.046 (0.047) | 0.101*** (0.008) |
| PDSI×Coal | 0.011 (0.009) | 0.027 (0.032) | 0.030 (0.027) | 0.006 (0.009) |
| PDSI×Natural gas | -0.029*** (0.008) | -0.021 (0.014) | 0.029 (0.033) | -0.045*** (0.011) |
| PDSI×Nuclear | 0.011 (0.015) | 0.018 (0.016) | 0.028 (0.028) | 0.008 (0.017) |
| PDSI×Solar | 0.024 (0.026) | 0.029 (0.026) | | |
| PDSI×Wind | 0.008 (0.014) | -0.012 (0.014) | 0.086 (0.059) | 0.074* (0.040) |
| PDSI×Geothermal | 0.007 (0.023) | 0.011 (0.023) | | |
| PDSI×Biomass | -0.003 (0.015) | 0.009 (0.022) | -0.055 (0.090) | -0.007 (0.021) |
| PDSI×Petroleum | -0.010 (0.008) | -0.013 (0.042) | 0.087** (0.041) | -0.012 (0.008) |
| PDSI×Other | -0.072*** (0.027) | 0.024 (0.077) | | -0.090*** (0.028) |
| CDD | 0.002*** (0.000) | 0.001*** (0.000) | -0.019 (0.035) | 0.002*** (0.000) |
| Observations | 334,824 | 90,300 | 13,020 | 231,504 |
| No. of plants | 3,986 | 1,075 | 155 | 2,756 |
| Within R-squared | 0.035 | 0.038 | 0.049 | 0.036 |
| Plant fixed effects? | Y | Y | Y | Y |
| Month-of-sample fixed effects? | Y | Y | Y | Y |

The dependent variable in each column is the inverse hyperbolic sine of net generation at the plant level. Each column represents regression results from before 2008 as a robustness check for the dramatic change in relative fuel prices induced by the natural gas boom. Standard errors in parentheses are clustered at the plant level. *** $p < 0.01$, ** $p < 0.05$, * $p < 0.1$. SOURCE: Authors' calculations.